

Fisica della Materia allo Stato Fluidico e di Plasma

2. Teoria della Orbite

Orbit Theory [Sturrock, Sec. 3.2]

3.2 Particle motion in electric and magnetic fields

We now consider the nonrelativistic motion of a charged particle moving through static uniform electric and magnetic fields. We see from the nonrelativistic form of (3.1.2) that the velocity components satisfy the equations

$$\frac{dv_{\parallel}}{dt} = \frac{q}{m} E_{\parallel} \quad (3.2.1)$$

and

$$\frac{d\mathbf{v}_{\perp}}{dt} = \frac{q}{m} \left(\mathbf{E}_{\perp} + \frac{1}{c} \mathbf{v}_{\perp} \times \mathbf{B} \right), \quad (3.2.2)$$

where \mathbf{v}_{\perp} is the part of the velocity vector normal to the magnetic field. Clearly, the particle accelerates freely in response to the electric field component along the magnetic field.

One method of determining the motion resulting from (3.2.2) is to consider the possibility that the transverse velocity can be separated into a constant component and a time-varying component, writing

$$\mathbf{v}_{\perp}(t) = \mathbf{v}_d + \mathbf{v}_g(t). \quad (3.2.3)$$

We will see that \mathbf{v}_d corresponds to 'drift' motion, and \mathbf{v}_g corresponds to 'gyro' motion.

Orbit Theory [Sturrock, Sec. 3.2]

The equation of motion (3.2.2) now becomes

$$\frac{d\mathbf{v}_g}{dt} = \frac{q}{m} \left(\mathbf{E}_\perp + \frac{1}{c} \mathbf{v}_d \times \mathbf{B} + \frac{1}{c} \mathbf{v}_g \times \mathbf{B} \right). \quad (3.2.4)$$

On separating out the time-independent and the time-dependent terms in this equation, we obtain

$$\mathbf{E}_\perp + \frac{1}{c} \mathbf{v}_d \times \mathbf{B} = 0 \quad (3.2.5)$$

and

$$\frac{d\mathbf{v}_g}{dt} = \frac{q}{mc} (\mathbf{v}_g \times \mathbf{B}). \quad (3.2.6)$$

On operating on (3.2.5) with a cross product with respect to \mathbf{B} , we find that

$$\mathbf{v}_d = c \frac{\mathbf{E} \times \mathbf{B}}{B^2}. \quad (3.2.7)$$

This shows that our nonrelativistic theory is valid only if $|\mathbf{E}| \ll |\mathbf{B}|$.

Curvature drift [Bellan 3.5.2]

- Write velocity as $\vec{v} = \vec{v}_\perp + \vec{v}_\parallel = \vec{v}_\perp + v_\parallel \hat{B}$

- Split the equation of motion as

$$\frac{d\vec{v}}{dt} = \frac{d\vec{v}_\perp}{dt} + \frac{d\vec{v}_\parallel}{dt} = \frac{d\vec{v}_\perp}{dt} + \frac{d(v_\parallel \hat{B})}{dt} = \frac{q}{mc} \vec{v}_\perp \times \vec{B}$$

- Then
$$\frac{d(v_\parallel \hat{B})}{dt} = \frac{dv_\parallel}{dt} \hat{B} + v_\parallel \frac{d\hat{B}}{dt}$$

- The first term is along the magnetic field, while

$$v_\parallel \frac{d\hat{B}}{dt} = v_\parallel \frac{\partial \hat{B}}{\partial s} \frac{ds}{dt} = v_\parallel^2 \frac{\partial \hat{B}}{\partial s} \quad [\text{see } \rightarrow \text{normal_and_binormal_vector.pdf}]$$

- where s is the distance along a magnetic field line. Now:

$$\frac{\partial \hat{B}}{\partial s} = (\hat{B} \cdot \nabla) \hat{B} = \left| \frac{\partial \hat{B}}{\partial s} \right| \hat{N} = \kappa \hat{N} \rightarrow (\text{cyl}) \rightarrow -\frac{\hat{R}}{R}$$

[see \rightarrow <http://mathworld.wolfram.com/Curvature.html>]

- Where $k =$ curvature, $R =$ radius of curvature $\kappa = \frac{1}{R}$

Curvature Drift

- The additional force will then be $\vec{F} = -mv_{\parallel}^2(\hat{B} \cdot \nabla)\hat{B} = mv_{\parallel}^2 \frac{\hat{R}_c}{R_c}$

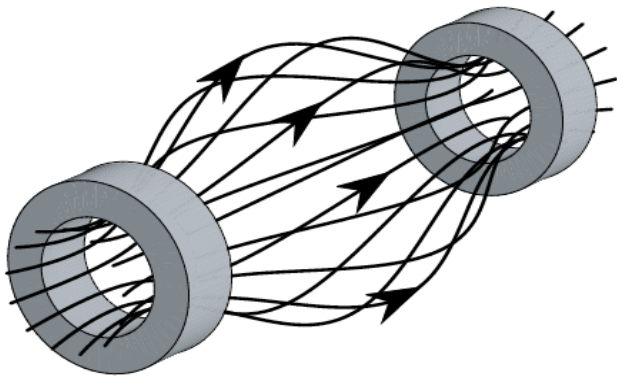
Adiabatic Invariants (Boyd page 28)

- Defining θ_0 to be the launching angle, particles with

$$\frac{\sin^2 \theta}{B} = \frac{\sin^2 \theta_0}{B_0} \quad \implies \quad \sin^2 \theta = \sin^2 \theta_0 \frac{B}{B_0} \leq 1$$

will keep going.

- If B has a maximum then particle having $\sin^2 \theta_0 \leq \frac{B_{\max}}{B_0}$ will proceed past the mirror.
- Conversely, particle with $\sin^2 \theta_0 > \frac{B_{\max}}{B_0}$ will be confined.



a) magnetic mirror

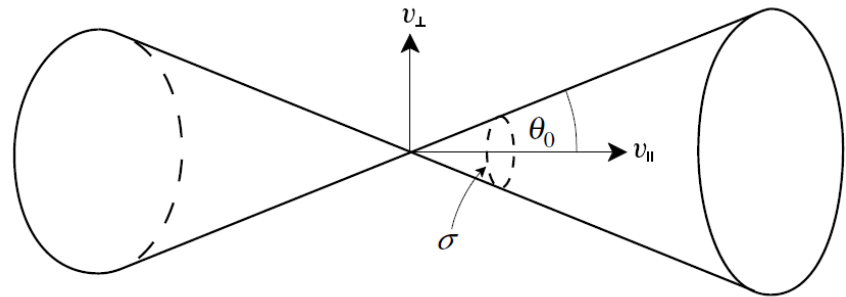


Fig. 2.8. Loss cone for a magnetic mirror. Particles with velocities within the cone will escape from the mirror.

Magnetic traps (Sturrock 43-45)

4.5 Magnetic traps

Consider the magnetic field configuration shown in Fig. 4.5, a configuration that is not assumed to have any particular type of symmetry. Consider the motion of a particle that starts out with a given velocity vector so that we know the initial value of the first adiabatic invariant, that is approximately constant. If the field is static, so that the particle energy is a constant, we know that the particle is reflected at points where the magnetic field strength takes the value B_R .

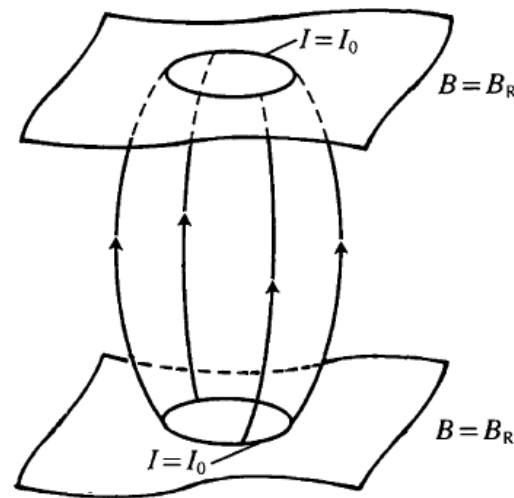


Fig. 4.5. A magnetic field configuration that does not have cylindrical symmetry but leads to the trapping of charged particles.

As we shall see in the next chapter, a particle tends to drift in an inhomogeneous magnetic field, so that it will migrate to other magnetic-field lines. If we now construct two surfaces on which $B=B_R$, and between which $B<B_R$, we know that the particle will be reflected at these two surfaces and trapped between the surfaces.

However, since we are assuming that the magnetic field is static, we can go further. We know, from the properties of the second adiabatic invariant, that the particle is constrained to move in such a way that $I=\text{constant}$, where I is defined by (4.4.16).

Hence, for each field line bounded by the two surfaces $B=B_R$, we may calculate the value of I . We may then identify the shell of magnetic-field lines for which $I=I_0$, where I_0 is the initial value of I . Hence we know that the particle will move in such a way that it is constrained to remain on the shell and that its motion is bounded by the two reflection surfaces. If the shell forms a closed surface, as indicated in Fig. 4.5, then the particle is constrained to remain on that surface, no matter what type of drift the magnetic-field gradients may imply.

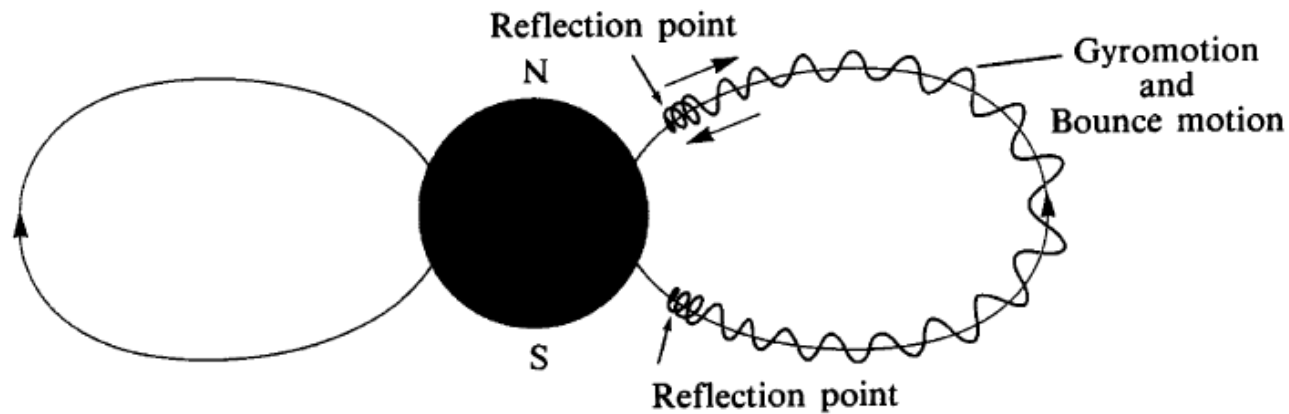


Fig. 4.6. A dipole-type magnetic field, such as that of the Earth, leads to particle trapping. Particles exhibit gyromotion around magnetic field lines, bounce motion along field lines between reflection points, and drift motion around the Earth.

Another example of a magnetic-field configuration that leads to trapping is that shown in Fig. 4.6, that of the magnetosphere of a body with a dipole magnetic field, such as the Earth. In this case, particles bounce from one reflection point to another in helical trajectories. In addition to this motion, there is (as we shall see in the next chapter) a drift around the earth due to the curvature of the magnetic field lines (curvature drift) and to the spatial variation of B with radius (gradient drift). Hence, for the particles trapped in the Earth's magnetosphere, there are three types of oscillations due to (a) the gyromotion, (b) the 'bounce' motion, and (c) the drift motion.

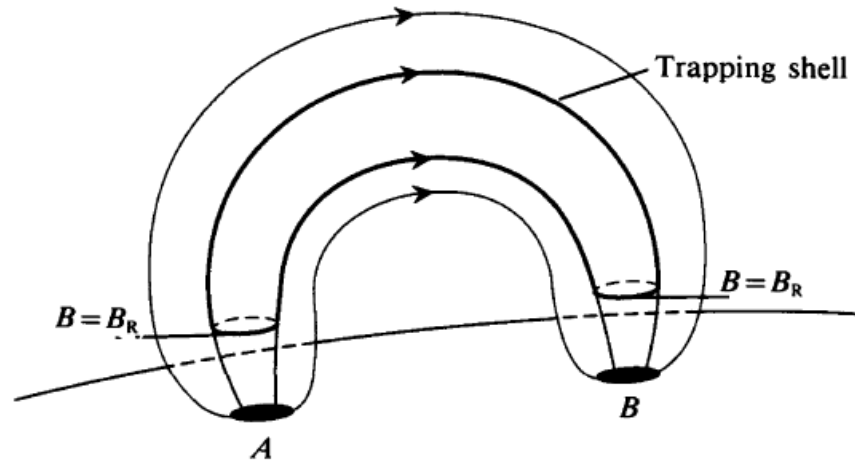


Fig. 4.7. A magnetic flux tube in a solar active region also provides for particle trapping. *A*: positive-polarity sunspot; *B*: negative-polarity sunspot.

Another example is the trapping of particles in the Sun's magnetic field, that is much more complex than the approximately dipole field of the earth. In an active region, that inevitably contains surface magnetic fields of opposite polarities, and typically contains at least one pair of sunspots of opposite polarities, part of the magnetic field will be as shown in Fig. 4.7. The Sun produces some radio bursts (stationary Type IV microwave radio bursts) that are initiated by flares and are believed to be due to gyrosynchrotron radiation. Hence, such flares indicate that mildly relativistic electrons are somehow trapped at coronal heights in an active region. We see from Fig. 4.7 that, here again, if the field is static it is reasonable that particles should be trapped in the region above the two reflection surfaces.

Accelerazione di particelle nello spazio

In uno specchio magnetico a simmetria assiale. (Figura 14 a) cariche che vengano iniettate nelle regioni di campo meno intenso tra le due compressioni e che abbiano angoli di iniezione al di fuori del cono di perdita, sono intrappolate tra due punti di specchio e si muovono avanti indietro tra di essi.

Sono tuttavia possibili specchi magnetici in diverse geometrie in particolare in geometria di dipolo magnetico, come quello terrestre, mostrato in Figura 14 b)

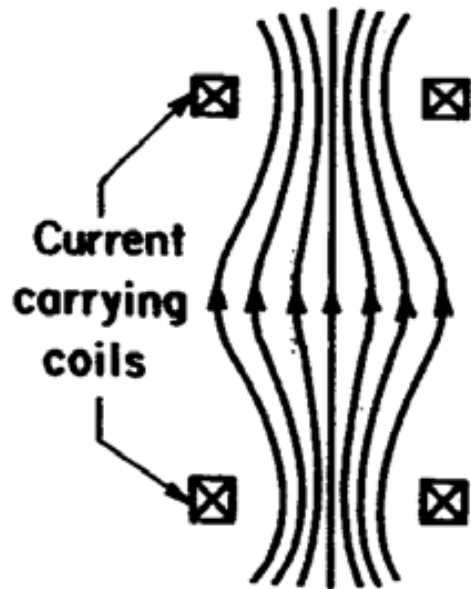


Figura 14 (a)

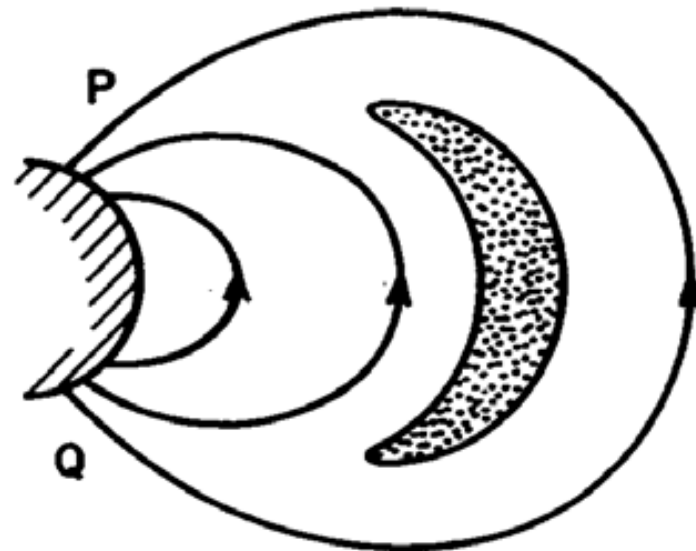


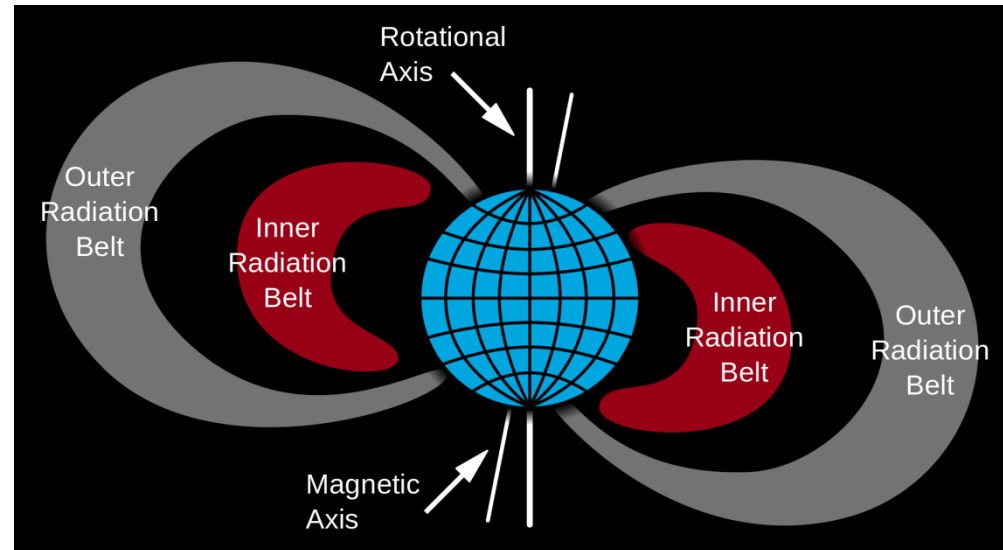
Figura 14 (b)

Anche in questo caso le linee di flusso si addensano verso i poli magnetici. Possiamo quindi pensare alle regioni polari come a due punti di specchio che danno origine a un confinamento magnetico: cariche iniettate (principalmente dal vento solare) in questo campo, al di fuori del cono di perdita, sono intrappolate tra le due regioni polari e si muovono avanti e indietro lungo le linee di flusso.

Data la forma delle linee di campo, sono presenti effetti di deriva di curvatura e di gradiente, che agiscono ambedue nella direzione azimutale. Il centro di guida delle particelle pertanto, nel suo moto tra i punti di specchio, si muove anche azimutalmente intorno all'asse del dipolo.

Cariche di segno opposto hanno moti azimutali contrari e danno quindi origine ad una corrente di deriva intorno al dipolo.

Questa configurazione è all'origine delle cosiddette fasce di Van Allen, scoperte intorno alla Terra nel 1958 dalle prime sonde spaziali Explorer e Sputnik, e costituenti la magnetosfera chiusa del nostro pianeta. Nelle fasce si trovano elettroni con energie tra 40 keV e 1 MeV e protoni con energie tra 100 keV e 1 GeV, che hanno punti di specchio a latitudini intorno ai 70° e si estendono tra 1.5 e 5 volte il raggio terrestre;

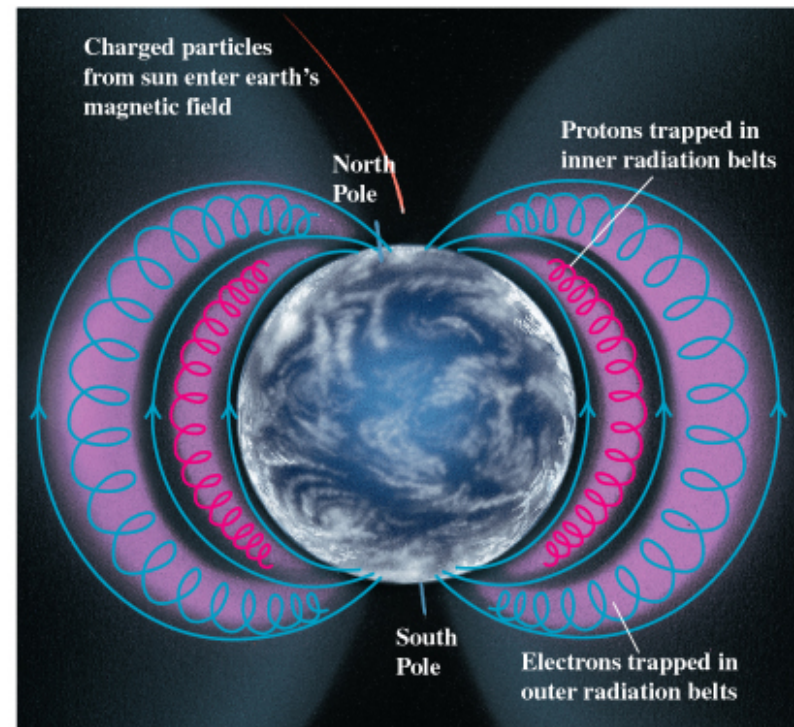


Le particelle di più bassa energia sono intrappolate nelle regioni più esterne, quelle di alta energia arrivano al bordo superiore della ionosfera, intorno a qualche centinaio di km. I flussi di particelle variano tra 10^4 e 10^7 particelle $\text{cm}^{-2} \text{s}^{-1}$.

Le fasce sono formate dalla cattura di particelle cariche del vento solare che penetrano nella magnetosfera, ma anche da cariche energetiche evaporate dalla ionosfera terrestre; intense fasce di elettroni sono state osservate formarsi a seguito delle esplosioni nucleari in atmosfera.

Le fasce variano irregolarmente in relazione all'attività solare; le particelle delle fasce si scaricano nei punti di specchio delle regioni polari per interazioni con le particelle dell'atmosfera terrestre, e sono responsabili dell'attività geomagnetica e delle aurore.

I moti di deriva generano la cosiddetta corrente ad anello che scorre lungo le fasce in direzione azimutale.



(a)

2.11 Adiabatic invariance and particle acceleration

Particle acceleration is of widespread interest in both laboratory and space plasmas. As an example we consider an idea originally put forward by Fermi (1949) to account for the very energetic particles ($O(10^{18}$ eV)) in cosmic radiation. How such enormous energies are attained is obviously a key question in cosmic ray theory. Fermi postulated that there are regions of space in which clumps of magnetic field of higher than average intensity occur with charged particles trapped between them. He argued that these magnetic clumps would not be static and trapped particles could be accelerated if such regions were approaching one another. By the same token, particles would lose energy in mirror regions that were separating. Fermi

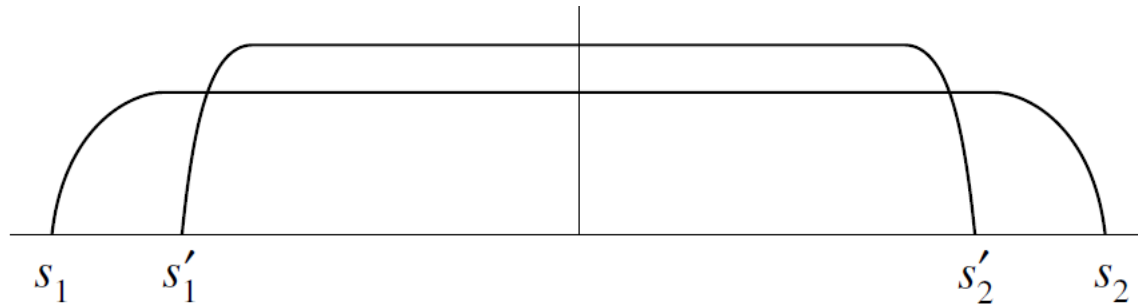


Fig. 2.11. Variation of v_{\parallel} between mirror points s_1 and s_2 . If the field maxima approach one another, so do the mirror points and at some later time the phase trajectory is given by the curve from s'_1 to s'_2 .

showed that the probability of head-on collisions was greater than that of overtaking collisions, their relative frequencies being proportional to $(v_{\parallel} + v_B)/(v_{\parallel} - v_B)$ where v_B is the velocity of the magnetic clump.

To see how Fermi acceleration works suppose a charged cosmic ray particle is trapped between two magnetic mirrors which move towards one another sufficiently slowly that J is a good adiabatic invariant. Suppose too that at $t = 0$ the coordinates of the mirror points in the phase space diagram, Fig. 2.11, are s_1 and s_2 , while at some later time, t' , they shift to s'_1 and s'_2 respectively. The invariance of J means that the area enclosed by the phase space orbit is constant. Denoting $s_1 - s_2$ by s_0 , $s'_1 - s'_2$ by s'_0 gives

$$v'_{\parallel} \simeq v_{\parallel} \frac{s_0}{s'_0}$$

where v_{\parallel} , v'_{\parallel} are the parallel components of velocity at the mid-plane at $t = 0$, $t = t'$, respectively. Then

$$W'_{\parallel} = \left(\frac{s_0}{s'_0} \right)^2 W_{\parallel}$$

and

$$W' = W'_{\perp} + W'_{\parallel} = \frac{m}{2} \left[v_{\perp}^2 + \left(\frac{s_0}{s'_0} \right)^2 v_{\parallel}^2 \right]$$

by making use of the invariance of μ_B (assuming the field is constant at the mid-plane). Thus the energy of a particle trapped between slowly approaching magnetic mirrors increases. As proposed originally, Fermi acceleration suffers from a serious limitation. For increasing v_{\parallel} , the pitch angle defined by (2.33) decreases so that at some stage a particle being accelerated falls into the loss cone and escapes, thus limiting the gain in energy.